Quantitative Measurement of Cross-Correlations between ^{15}N and ^{13}CO Chemical Shift Anisotropy Relaxation Mechanisms by Multiple Quantum NMR

Maurizio Pellecchia,[†] Yuxi Pang,[†] Lincong Wang,[†] Alexander V. Kurochkin,[†] Anil Kumar,[†,∥,⊥] and Erik R. P. Zuiderweg*[,†,‡,§]

Contribution from the Biophysics Research Division, Department of Biological Chemistry, and Department of Chemistry, The University of Michigan, 930 North University Avenue, Ann Arbor Michigan 48109, and Parke-Davis Pharmaceutical Research, 2800 Plymouth Road, Ann Arbor, Michigan 48105

Received April 12, 1999. Revised Manuscript Received August 6, 1999

Abstract: This paper describes an experiment that allows the quantitative measurement of the CSA−CSA cross-correlation between backbone ^{15}N and ^{13}CO nuclei in uniformly enriched proteins. The CSA−CSA cross-correlation is obtained from the cross-peak intensity ratios of the double- and the zero-quantum components observed with a modified triple-quantum 2D CT-HNCO experiment. In addition, the $^{1}H^{N}-^{15}N/^{1}H^{N}-^{13}CO$ dipole−dipole cross-correlation was measured without relying on resolved scalar couplings using a complementary quantum 2D CT-HNCO experiment. The cross-correlation rates measured for the protein binase (12.3 kDa) were obtained with high precision but show a surprisingly large range of values. Calculations show that this range is at least partially caused by dynamical processes. The potential use of this information to characterize internal anisotropic motion is discussed.

Recent years have witnessed increasing interest in the observation of various forms of cross-correlations,[1−6] i.e., cross-correlated fluctuations of different dipolar couplings (DD) and of dipolar couplings and chemical shielding anisotropy (CSA). These interference effects are being studied because of their disturbing effect upon conventional measurements of heteronuclear relaxation rates in proteins[7] and their correlation with local internal motion.[8−14] In addition, measurements of cross-correlations have been successfully employed to determine CSA tensors or angles subtended by dipolar vectors or by dipolar and CSA vectors. In some very elegant applications, these angles have been used to indirectly determine dihedral angles in proteins[15,16] or to determine sugar ring puckering.[17] Finally, the phenomenon of differential line broadening caused by DD−CSA cross-correlations inspired the development of a series of novel double and triple resonance experiments with attenuated ^{15}N and ^{13}C T_2 relaxation (TROSY)[18,19] and their successful implementation has been recently demonstrated in several different applications.[20−23]

In addition to DD−DD and DD−CSA cross-correlation effects, CSA−CSA cross-correlation, is anticipated from a theoretical basis. The possibility of a CSA−CSA cross-correlated relaxation was first supposed by Vold and Vold.[2] Later Werbelow,[24] Konrat and Sterk,[25] and more recently Kumar

* Corresponding author. Telephone: (734) 936-3850. Fax: (734) 764-3323. E-mail: zuiderwe@umich.edu.

† Biophysics Research Division, The University of Michigan.

‡ Department of Biological Chemistry, The University of Michigan.

§ Department of Chemistry, The University of Michigan.

∥ Parke-Davis Pharmaceutical Research.

⊥ Present address: Department of Physics, Indian Institute of Science, Bangalore, 560 012 India.

(1) Werbelow, L. G. In *Encyclopedia of Nuclear Magnetic Resonance*; Grant, D. M., Harris, R. K., Eds; Wiley: London, 1996; Vol. 6, pp 4072−4078.

(2) Vold, R. L.; Vold, R. R. *Prog. Nucl. Magn. Reson. Spectrosc*. **1978**, *12*, 79−133.

(3) Goldman, M. *J. Magn. Reson*. **1984**, *60*, 437−452.

(4) Tolman, J. R.; Prestegard, J. H. *J. Magn. Reson*. **1995**, *106*, 97−100.

(5) Kumar, A.; Madhu, P. K. *Concepts Magn. Reson*. **1996**, *8*, 139−160.

(6) Daragan, V. A.; Mayo, K. H. *Prog. Nucl. Magn. Reson. Spectrosc*. **1997** *31*, 63−105.

(7) Boyd, J.; Hommel, U.; Campbell, I. D. *Chem. Phys. Lett*. **1990**, *174*, 477−482.

(8) Tjandra, N.; Bax, A. *J. Am. Chem. Soc*. **1997**, *119*, 8076−8082.

(9) Tessari, M.; Vis, H.; Boelens, R.; Kaptein, R.; Vuister, G. W. *J. Am. Chem. Soc.* **1997**, *119*, 8985−8990.

(10) Tessari, M.; Mulder, F. A. A.; Boelens, R.; Vuister, G. W. *J. Magn. Reson*. **1997**, *127*, 128−133.

(11) Ghose, R.; Prestegard, J. H. *J. Magn. Reson*. **1998**, *134*, 308−314.

(12) Ghose, R.; Huang, K.; Prestegard, J. H. *J. Magn. Reson*. **1998**, *135*, 487−499.

(13) Fischer, M. W. F.; Zeng, L.; Pang, Y.; Hu, W.; Majumdar, A.; Zuiderweg, E. R. P. *J. Am. Chem. Soc.* **1997**, *119*, 12629−12634.

(14) Brutscher, B.; Srynnikov, N. R.; Bremi, T.; Brüschweiler, R.; Ernst, R. R. *J. Magn. Reson*. **1998**, *130*, 346−351.

(15) Reif, B.; Hennig, M.; Griesinger, C. *Science* **1997**, *276*, 1230−1233.

(16) Yang, D.; Konrat, R.; Kay, L. E. *J. Am. Chem. Soc*. **1997**, *119*, 11938−11940.

(17) Griesinger, C. Report from the Keystone Symposium, Breckenridge, CO, 1999.

(18) Pervushin, K.; Rieck, R.; Wider, G.; Wüthrich, K. *Proc. Natl. Acad. Sci. U.S.A.* **1998**, *94*, 12366−12371.

(19) Pervushin, K.; Rieck, R.; Wider, G.; Wüthrich, K. *J. Am. Chem. Soc.* **1998**, *120*, 6384−6400.

(20) Salzmann, M.; Pervushin, K.; Wider, G.; Senn, H.; Wüthrich, K. *Proc. Natl. Acad. Sci. U.S.A.* **1998**, *95*, 13585−13590.

(21) Pervushin, K.; Ono, A.; Fernandez, C.; Szyperski, T.; Kainosho, M.; Wüthrich, K. *Proc. Natl. Acad. Sci. U.S.A.* **1998**, *95*, 14147−14151.

(22) Pellecchia, M.; Sebbel, P.; Hermanns, U.; Glockshuber, R.; Wüthrich, K. *Nat. Struct. Biol.* **1999**, *6*, 336−339.

(23) Brutscher, B.; Boisbouvier, J.; Pardi, A.; Marion, D.; Simorre, J. P. *J. Am. Chem. Soc*. **1998**, *120*, 11845−11851.

(24) Werbelow, L. G. *J. Magn. Reson*. **1987**, *71*, 151−153.

10.1021/ja991155d CCC: $18.00
Published on Web 09/18/1999

and Kumar,[26] showed that the relaxation of the double- and zero-quantum coherences of two spins is affected by the cross-correlation of their respective CSA tensors. While this paper was under revision, two different groups also described the differential line-broadening effect in zero-and double-quantum coherences for $^{15}N-{}^{1}H^{N}$ nuclei due to CSA−CSA cross-correlation.[27]

In this paper we will show that the CSA−CSA cross-correlation between backbone amide nitrogen (^{15}N) and carbonyl (^{13}CO) nuclei ($CC_{N,C}$) is manifested in differential relaxation in double- and zero-quantum coherences detected in modified 2D CT-HNCO experiments. In addition, we will show that the cross-correlation between $^{1}H^{N}-{}^{15}N$ and $^{1}H^{N}-{}^{13}CO$ dipole−dipole interactions ($CC_{NH,CH}$) can be also measured from these experiments. While it is difficult to separate the dynamic and the structural contribution on the values of the measured cross-correlations, we found our results particularly interesting for the following reasons. First, the potential of nuclear spin cross-correlated relaxation as a source of dynamic information is particularly intriguing as it relates to the way in which the two interaction vectors follow one another during reorientation. In addition, the novel CSA−CSA cross-correlation may provide information on chemical shielding tensors and their relative orientation, which may in turn provide useful information on dihedral angles and hydrogen bonding. Moreover, the large differential line broadening observed in the multiple quantum spectrum of backbone ^{15}N and ^{13}CO nuclei, due to their CSA−CSA cross-correlation, may represent at higher magnetic fields, a novel means to attenuate transverse relaxation in a fashion alternative (and/or complementary) to the TROSY principle. The fact, finally, that the CSA−CSA cross-correlation does not depend on the distance between the nuclei involved but only on the possibility to generate multiple quantum coherence between them opens a window on a myriad of multiple quantum experiments with the potentialities listed above.

Theory

The experimental 2D-CT HNCO schemes used to measure the ^{15}N, ^{13}CO CSA−CSA cross-correlation ($CC_{N,C}$) are reported in Figure 1. In the following discussion we will indicate with *H* the amide proton, with *N* the amide nitrogen, and with *C* the carbonyl carbon nuclei. The magnetization transfer is very similar to the original CT-HNCO experiment used for backbone resonance assignments; [28] therefore we will focus only on the essential part of our experiment that is the central constant time period of length Δ. At the beginning of this time period the two-spin coherence term $2N_xC_x$ is present in the spin-density operator. This term can be decomposed into zero-quantum coherences $(^1/_2)(N_+C_- + N_-C_+)$ and double-quantum coherences $(^1/_2)(N_+C_+ - N_-C_-)$. These coherences experience during the constant time evolution period Δ (Figure 1A) auto- and cross-correlated relaxation together with chemical shift evolution. Amide proton and alpha carbon are decoupled by 180° pulses in the middle of the constant time evolution period Δ (Figure 1A). The 180° pulses in the middle of the Δ period also cause the relaxation of the doublet components of the zero- and double-quantum coherences to interchange their relaxation

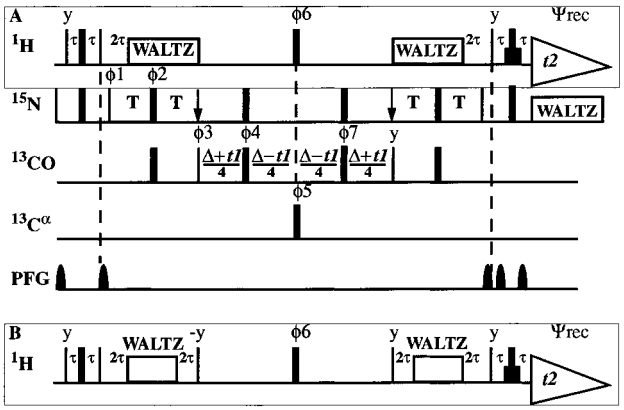

Figure 1. (A) Pulse sequence for determination of transverse ^{13}CO and ^{15}N CSA−CSA cross-correlation rates ($CC_{N,C}$) and $^{1}H^{N}-{}^{15}N$ and $^{1}H^{N}-{}^{13}CO$ dipole−dipole cross-correlation rates ($CC_{NH,CH}$). Narrow and thin bars represent 90 and 180° rf pulses, respectively. Unless specified otherwise, pulse phases are along the *x* axis. The durations of the ^{13}-CO and $^{13}C^{\alpha}$ pulses have been optimized not to interfere with each other. Pulsed field gradients are half-sinebell shaped with 1 ms duration and strengths of $g_1 = 20$ G/cm, $g_2 = 40$ G/cm, $g_3 = 30$ G/cm, $g_4 = 50$ G/cm. The delays are: $\tau = 2.7$ ms, $T = 11.0$ ms, and $\Delta = 22$ ms. States-TTPI quadrature detection is achieved by incrementing $\phi 3$ so that cross-peaks at $\omega_C \pm \omega_N$ were observed. To reduce the resonance overlap between double- and zero-quantum cross-peaks the ^{15}N carrier frequency was shifted to the edge of the ^{15}N spectral envelope prior chemical shift evolution (indicated by vertical arrows), and subsequently shifted back to the center of the spectrum. Alternative schemes for this task have also been proposed.[13] ^{15}N decoupling during t_2 was achieved with a 1.25 kHz WALTZ-16 decoupling sequence. Water suppression was achieved with a WATERGATE scheme.[45] Phase cycle: $\phi_1 = x, x, -x, -x$; $\phi_2 = x, x, -x, -x$; $\phi_3 = -y, y$; $\phi_4 = 4(x), 4(y)$; $\phi_5 = 16(x), 16(-x)$; $\phi_6 = 16(x), 16(-x)$; $\phi_7 = 8(x), 8(y)$; $\Psi_{rec} = x, -x, -x, x, 2(-x, x, x, -x), x, -x, -x, x$. (B) The pulse scheme is identical to the one in (A) except for the two delays 2τ ($\tau = 2.7$ms) and two 90° proton pulses just before and after the chemical shift evolution time period, Δ. Phase cycle: $\phi_1 = x, x, -x, -x$; $\phi_2 = x, x, -x, -x$; $\phi_3 = -y, y$; $\phi_4 = 8(x), 8(y)$; $\phi_5 = 16(x), 16(-x)$; $\phi_6 = 4(x), 4(y)$; $\phi_7 = 16(x), 16(y)$; $\Psi_{rec} = x, -x, -x, x, 2(-x, x, x, -x), x, -x, -x, x, -x, x, x, -x, 2(x, -x, -x, x), -x, x, x, -x$. For nonperdeuterated proteins, to reduce losses due the homonuclear *J* coupling evolution during the delay, Δ, it is advisable to substitute the ^{1}H 180° pulse in the middle of the chemical shift evolution with an amide proton-selective 180° pulse.

rates, retaining the secular approximation, and yield an average relaxation of the components, canceling various CSA/dipole−dipole cross-correlated relaxation mechanisms arising mainly from the amide proton. With amide proton decoupling the two doublet components of the zero- and double-quantum coherences are degenerate and the logarithmic ratio between the cross-peaks intensities of the double- (I_{DQ}) and zero-quantum (I_{ZQ}) coherences is given by:[25]

$$(\Delta)^{-1} \ln(I_{ZQ}/I_{DQ})_A = -2R_{NC,NC}(\omega N - \omega C) + 12R_{NC,NC}(\omega N + \omega C) + 2CC_{NH,CH}(0) + 2CC_{NH,CH}(\omega H) + 2CC_{NC}(0) \quad (1)$$

where $R_{NC,NC}(\omega)$ is the transverse autorelaxation rate due to fluctuations at frequencies (ω) for the $^{15}N-{}^{13}CO$ dipole interaction, $CC_{NH,CH}(\omega)$ represents the transverse cross-correlated relaxation rate of the $^{1}H^{N}-{}^{15}N$ and internuclear $^{1}H^{N}-{}^{13}CO$ vectors due to fluctuations at frequencies (ω), and $CC_{NC}(\omega)$ is the transverse cross-correlation relaxation rate of ^{15}N and ^{13}CO nuclei chemical shielding anisotropy at frequencies (ω).

(25) Konrat, R.; Sterk, H. *Chem. Phys. Lett.* **1993**, *203*, 75−81.
(26) Kumar, P.; Kumar, A. *J. Magn. Reson.* **1996**, *119A*, 29−37.
(27) (a) Norwood, T. J.; Tillett, M. L.; Lian, L. Y.; *Chem. Phys. Lett.* **1999**, *300*, 429−434. (b) Pervushin, K.; Wider, G.; Rieck, R.; Wüthrich, K. *Proc. Natl. Acad. Sci. U.S.A.* **1999**, *96*, 9607−9612.
(28) Grzesiek, S.; Bax, A. *J. Magn. Reson.* **1992**, *96*, 432−440.

Assuming isotropic motion, the various rates of eq 1 can be expressed by:[3,29a]

$$R_{NC,NC}(\omega N + \omega C) = ({}^1/_8)(\mu_o/4\pi)^2(h/2\pi)^2\gamma_C{}^2\gamma_N{}^2(r_{NC}{}^{-6})[2\tau c/5(1 + (\omega_C + \omega_N)^2\tau_c{}^2)] \quad (2a)$$

$$R_{NC,NC}(\omega N - \omega C) = ({}^1/_8)(\mu_o/4\pi)^2(h/2\pi)^2\gamma_C{}^2\gamma_N{}^2(r_{NC}{}^{-6})[2\tau c/5(1 + (\omega_C - \omega_N)^2\tau_c{}^2)] \quad (2b)$$

$$CC_{NH,CH}(\omega H) = [({}^1/_4)(\mu_o/4\pi)^2(h/2\pi)^2]\gamma_C\gamma_H\gamma_N\gamma_H(r_{HN}{}^{-3})(r_{CH}{}^{-3})P_2 \cos(\theta)\, 6\tau_c/5(1 + \omega_H{}^2\tau_c{}^2) \quad (2c)$$

$$CC_{NH,CH}(0) = [({}^1/_4)(\mu_o/4\pi)^2(h/2\pi)^2]\gamma_C\gamma_H\gamma_N\gamma_H(r_{HN}{}^{-3})(r_{CH}{}^{-3})P_2 \cos(\theta)\, 8\tau_c/5 \quad (2d)$$

$$CC_{N,C}(0) = ({}^2/_{18})\gamma_N\gamma_C B_o{}^2(\Delta\sigma_N)\{[\sigma_{22} - \sigma_{33}][P_2\cos(\theta_{11} + 90)] + [\sigma_{11} - \sigma_{33}][P_2\cos(\theta_{11})]\}8\tau_c/5 \quad (2e)$$

In eq 2, r_{HN} and r_{CH} denote the $^1H^{N-N}$ and $^1H^N - ^{13}CO$ internuclear distances, respectively. $P_2\cos(\theta) = 0.5(3\cos^2\theta - 1)$ where θ represents the angle between these two vectors. $\Delta\sigma_N$ denotes the difference between the parallel and perpendicular components of the axially symmetric ^{15}N chemical shielding tensors. $\sigma_{11} - \sigma_{33}$ and $\sigma_{22} - \sigma_{33}$ are the principal components of the rhombic ^{13}CO chemical shielding tensor, expressed as the sum of two axially symmetric tensors and the corresponding angles θ_{11} and $(\theta_{11} + 90)$ define the orientations of each of these tensors with respect to the unique axis of the ^{15}N chemical shielding tensor. τ_c is the overall isotropic correlation time of the molecule. Note that the coefficients of eq 1 differ from those reported in ref 25 because of the different coefficients used in the definition of the spectral density functions. However, the two formulations are numerically identical.

Assuming standard bond length and angles, the value of the various rates can be easily calculated from eq 2. For biological macromolecules the rates of eqs 2a,b,c are generally much smaller than those of eqs 2d,e. The protein binase (12.3 kDa) used in our study, reorients in solution with an overall correlation time of 6.0 ns at 30 °C.[29b] It can be easily calculated that the terms containing spectral density functions at higher frequencies (eqs 2a,b,c) represent less than 4% of the cross-correlation terms containing spectral density functions at zero frequency (eqs 2d,e). The former terms can thus be neglected, and eq 1 can be written as:

$$(\Delta)^{-1}\ln(I_{ZQ}/I_{DQ})_A = 2CC_{NH,CH}(0) + 2CC_{NC}(0) \quad (3)$$

In an additional experiment we can separate the contribution of the CSA−CSA cross-correlation from the $^1H^N-^{15}N$, $^1H^N-^{13}CO$ dipole−dipole cross-correlation. This is achieved with the pulse scheme of Figure 1B, in which prior to the constant time evolution period Δ, triple-quantum coherence of the type $4H_xN_xC_x$ is generated, by application of another 90° pulse on the protons, but the evolution of only the ^{15}N and ^{13}C double- and zero-quantum coherences takes place during delta period. The generation of the three-spin coherence between the amide proton and ^{15}N and ^{13}C ensures that the $J(0)$ dipolar relaxation between these nuclei is eliminated.[30] Consequently the dipolar term in eq 3 can be dropped and we obtain

$$(\Delta)^{-1}\ln(I_{ZQ}/I_{DQ})_B = 2CC_{NC}(0) \quad (4)$$

where the subscript B is underlining that the cross-peaks intensity ratios are taken from the experiment of Figure 1B.

In principle, dipolar cross-correlation terms of the type given in eqs (2c and d) involving other nuclei, e.g. the alpha proton and alpha carbon, are not suppressed in the triple-quantum experiment. However, it can be easily calculated that their contributions can be neglected in good approximation as the dipolar interactions themselves are small. Therefore ^{15}N, ^{13}CO CSA−CSA cross-correlation can be directly measured according to eq 4 from the cross-peaks intensity ratio between the zero- and double-quantum components of a triple-quantum spectrum recorded with the experimental scheme reported in Figure 1B. The cross-correlation rate between the $^1H^N-^{15}N$ and $^1H^N-^{13}CO$ dipole−dipole interaction can than be obtained from the difference of the cross-peaks intensity ratios measured in spectra recorded with both schemes of Figure 1, according to eqs 3 and 4. It should be pointed out that the cross-correlation rates determined by these experiments are obtained without relying on resolved scalar coupling.

Results and Discussion

Figure 2 shows representative ^{13}CO,^{15}N zero- and double-quantum cross-peaks measured with the experimental schemes reported in Figure 1 for the protein binase (12.3 kDa) from *Bacillus intermedius*. The resulting values of the $CC_{NC}(0)$ and $CC_{NH,CH}(0)$ rates measured from the cross-peak intensity ratios according to eqs 3 and 4 are plotted versus the amino acid sequence of binase in Figure 3. ^{15}N, ^{13}CO CSA−CSA cross-correlation rates vary between -5.23 and $1.18\ s^{-1}$ with an average value of $-2.27 \pm 1.37\ s^{-1}$, while and $^1H^N-^{15}N$ and $^1H^N-^{13}CO$ dipole−dipole cross-correlation rates vary between -3.82 and $-0.10\ s^{-1}$ with an average value of $-2.02 \pm 0.78\ s^{-1}$. Although the average values for both cross-correlations fall within the expected ranges calculated with eq 2 (see below), the large deviations along the polypeptide chain are quite unexpected. These variation are not caused by experimental uncertainties, which are on average less than 10% (see legends to Figures 2 and 3). Neither can the variations be correlated to the secondary structure of the protein (see Figure 3). Attempts to correlate the variations with hydrogen bonding patterns as observed in the crystal structure for binase[34] were also unsuccessful.

The observed variations can depend on local internal anisotropic motion, on variations of tensors and angles between tensors, or combinations thereof. Current knowledge about protein ^{15}N and ^{13}C CSA tensors in solution seems to indicate that ^{15}N tensors are subject to much larger variations than ^{13}C

(29) (a)Fischer, M. W. F.; Majumdar, A.; Zuiderweg, E. R. P. *Prog. Nucl. Magn. Reson. Spectrosc.* **1998**, *33*, 207−272. (b)Pang, Y.; Zuiderweg, E. R. P., unpublished data.

(30) Cavanagh, J.; Fairbrother, W. J.; Palmer, A. G.; Skelton, N. J. *Protein NMR Spectroscopy*; Academic Press: New York, 1996.
(31) Sitkoff, D.; Case, D. A. *Prog. Nucl. Magn. Reson. Spectrosc*. **1998**, *32*, 165−190.
(32) Fushman, D.; Tjandra, N.; Cowburn, D. *J. Am. Chem. Soc.* **1999**, *120*, 10947−10952.
(33) Asakawa, N.; Kuroki, S.; Kurosu, H.; Ando, I.; Shoji, A.; Ozaki, T. *J. Am. Chem. Soc.* **1992**, *114*, 3261−3265.
(34) Pavlovsky, A. G.; Vagin, A. A.; Vainstein, B. K.; Chepurnova, M. K.; Karpeisky, M. Y. *FEBS Lett.* **1983**, *162*, 167−170.

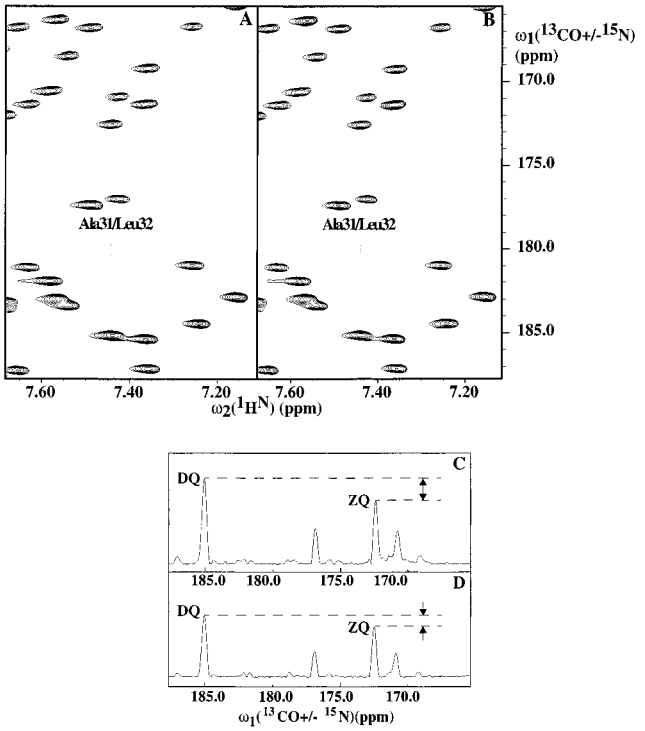

Figure 2. Representative region of the 2D CT-HNCO type spectra recorded with (A) the pulse scheme of Figure 1A, and (B), the pulse scheme of Figure 1B. Panels (C) and (D) show traces along ω_2 taken at the HNCO resonance of the residues Ala31-Leu32 from the spectra in (A) and (B), respectively. The spectra were acquired on a Bruker AMX500 spectrometer operating at 500 MHz ^{1}H frequency equipped with four rf channels and a Nalorac 8 mm triple resonance probe with a shielded *z*-gradient coil. All spectra were measured at 303 K with a 1.0 mM sample of ^{15}N,^{13}C-labeled binase (12.3 kDa) from *B. intermedius*. The measuring times for the two experiments were 12 and 24 h, respectively. The assignments were extended from ref 46. The smaller cross-peaks seen in the traces are caused by incompletely suppressed single-quantum coherences and their quadrature images that occur at known locations in the spectra. Quantitative analysis was only carried out for those double- and zero-quantum cross-peaks that were known to be unaffected by the single-quantum peaks.

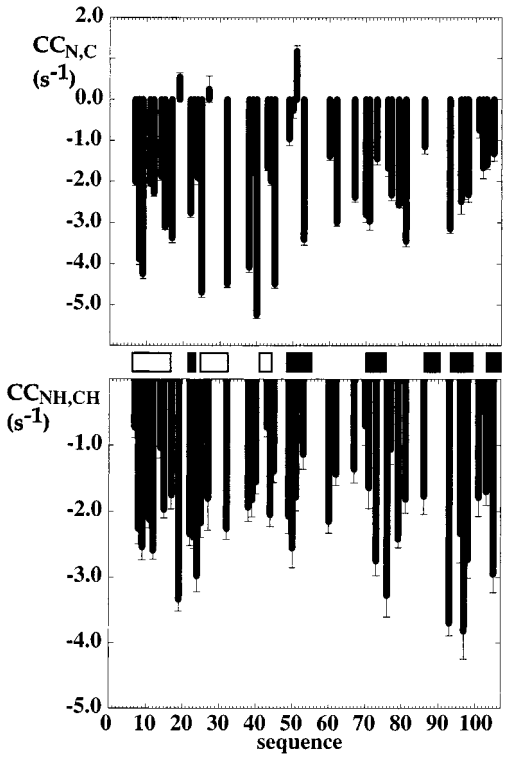

Figure 3. Plot versus the amino-acid sequence of (A) the ^{15}N−^{13}CO CSA−CSA cross-correlation rates $CC_{N,C}(0)$, and (B) the ^{1}H^N−^{15}N and ^{1}H^N−^{13}CO dipole−dipole cross-correlation rates $CC_{NH,CH}(0)$ measured for the protein binase (12.3 kDa) for well-resolved cross-peaks. The error bars were obtained as follows. The intrinsic experimental error was estimated from the signal peak height-to-noise ratio, where care was taken to analyze only those signals unaffected by single quantum peaks (see legend to Figure 2). The baseline was defined in areas where such single-quantum peaks did not occur. The intrinsic experimental errors were 0.4% on average, and were propagated through eqs 3 and 4 according to standard error theory.[47] Additional systematic errors arise from spectral density terms at higher frequencies that contribute for about 4% (see text), and from magnetic field inhomogeneities. The latter contribution has been experimentally estimated to account for an additional 4% uncertainty. The secondary structure elements for binase are also indicated with empty and filled boxes for α-helices and β-strands, respectively.

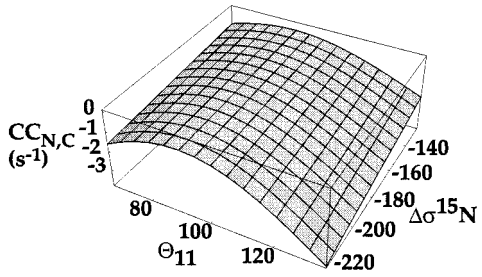

Figure 4. Dependence of the CSA−CSA cross-correlation $CC_{N,C}(0)$ on the variations of ^{15}N chemical shielding tensors $\Delta\sigma_N$,[32] and intervector angles θ_{11} between the ^{13}CO tensors and the unique axis of the ^{15}N tensors, according to eq 2e. ($\sigma_{22} - \sigma_{33}$) and ($\sigma_{11} - \sigma_{33}$) were set to −88 and −154 ppm, respectively.[29] The angle θ_{11} was varied to account for the reported variations of the angles between the unique axis of the ^{15}N CSA tensor and the ^{1}H^N−^{15}N bond vector,[32] between the ^{13}CO σ_{22} tensor and the ^{13}C═O bond vector,[33] and for small deviations from peptide plane planarity (see text).

tensors.[31] A computation of the dependence of $CC_{NC}(0)$ on $\Delta\sigma_N$ and θ_{11} according to eq 2e is shown in Figure 4. $\Delta\sigma_N$ defines the difference between the parallel and perpendicular components of the ^{15}N chemical shielding tensors, and θ_{11} defines the orientation of one of the principal components of the ^{13}CO chemical shielding tensors with respect to the unique axis of the ^{15}N chemical shielding tensor. The angle θ_{11} was varied to comprise the reported variation of the angles between the unique axis of the ^{15}N CSA tensor and the ^{1}H^N−^{15}N bond vector between 6 and 26°,[32] the variation of the angle between the ^{13}CO σ_{22} tensor and the ^{13}C═O bond vector between −3.6 to +5.8°,[33] and the deviations from planarity (± 7°) of the peptide bond as observed in the crystal structure of binase.[34] Figure 4 demonstrates quite a large dependence on variations of the intervector angle but a relatively small dependence on variations of $\Delta\sigma_N$. Although such (putative) structural variations would thus explain the majority of the observed variations in $CC_{NC}(0)$ cross-correlations, it still cannot account for the even larger variations observed for binase in Figure 3A, where, for example, some residues display inversion of the sign of the cross-correlations.

The analysis of the $CC_{NH,CH}(0)$ cross-correlation rates (Figure 3B) is, from a theoretical basis, more simple since its values depend only on distances and angles that should not be subject to large variations (see eq 2d). This dipole−dipole cross-correlation rate is thus expected to be constant, and should, considering standard bond lengths and angles, amount to −2.0

s^{-1}. However, also in this case the deviations from the average value are very large, and cannot be explained from geometrical arguments.

Recent observations based on both NMR data and molecular dynamics simulations show that backbone ^{15}N and ^{13}CO spin motion is dominated by anisotropic axial fluctuations of the peptide planes along the $^{13}C^{\alpha}(i-1)-^{13}C^{\alpha}(i)$ axes[29,35−38] ("crank-shaft" motion). For the measured CSA−CSA cross-correlation, such a motion would affect the cross-correlation term involving the ^{13}CO ($\sigma_{22}-\sigma_{33}$) sub-tensor (cf. eq 2e) differently than the term involving the ^{13}CO ($\sigma_{11}-\sigma_{33}$) sub-tensor.[33] To gain more insight, we calculated the effect of anisotropic local motion around three different axes on the cross-correlations. This was carried out by replacing the terms $P_2\cos(\theta)\,2\tau_c/5$ in eqs 2d and 2e with "model free" spectral density functions $J^{ij}(\omega)$ for (cross) correlation between relaxation vectors i and j accounting for local motion:[6, 13, 29]

$$J^{ij}(\omega) \cong {}^{2}/_{5}\left\{\frac{S_{ij}\tau_c}{1+(\omega\tau_c)^2}\right\} \tag{5}$$

The quantity S_{ij} is the product of the (nonsquared) order parameters S_i and S_j of the vectors i and j, i.e., the "cross-correlation order parameter" ($|P_2(\cos\theta_{ij})| \geq |S_{ij}| \geq 0$) which is sensitive to local motions. The cross-correlation order parameter can be computed from

$$S_{ij} = \frac{4\pi}{5}\sum_{m=-2}^{2}\langle Y_{2m}(\theta_i,\varphi_i)\rangle\langle Y^{*}_{2m}(\theta_j,\varphi_j)\rangle \tag{6}$$

where

$$\langle Y_{2m}(\theta_{ii},\varphi_{ii})\rangle = \int_0^{2\pi}\int_0^{\pi} Y_{2m}(\theta_{ii},\varphi_{ii})\,P_{ii}(\theta_{ii},\varphi_{ii})\sin\theta\,\mathrm{d}\theta\,\mathrm{d}\varphi \tag{7}$$

$P(\theta_i,\varphi_i)$ is a probability descriptor of the local motion of the relaxation vector i; similar definitions apply to the vector j. The functions $Y_{2m}(\theta,\varphi)$ are normalized spherical harmonics. The probability was modeled[29,14] as a Gaussian distribution of rotational states of these vectors around the direction of the motions for the range ±1 standard deviation as indicated in Figure 5.

The figure indicates that differences in extent and direction of anisotropic local motions can cause significant differences in the $CC_{NC}(0)$ (Figure 5A) and $CC_{HN,CH}(0)$ (Figure 5B) cross-correlation rates. From Figure 5A, one can observe that rapid "crank-shaft" rotational fluctuations of about ±30° around an axis parallel to σ_{11} would indeed cause an inversion of sign in the $CC_{NC}(0)$ cross-correlation rates. Local motion affects cross-correlation rates differently when different choices for the values of the CSA tensors, and especially the directions of their principal axes, are made (simulations not shown). In general the effect is that the presence of local anisotropic motion will greatly amplify the spread in cross-correlations which can initially be caused by a "static" spread in tensors and angles as shown in Figure 4. Large anisotropic rotational fluctuations of the peptide plane do account for most of the otherwise

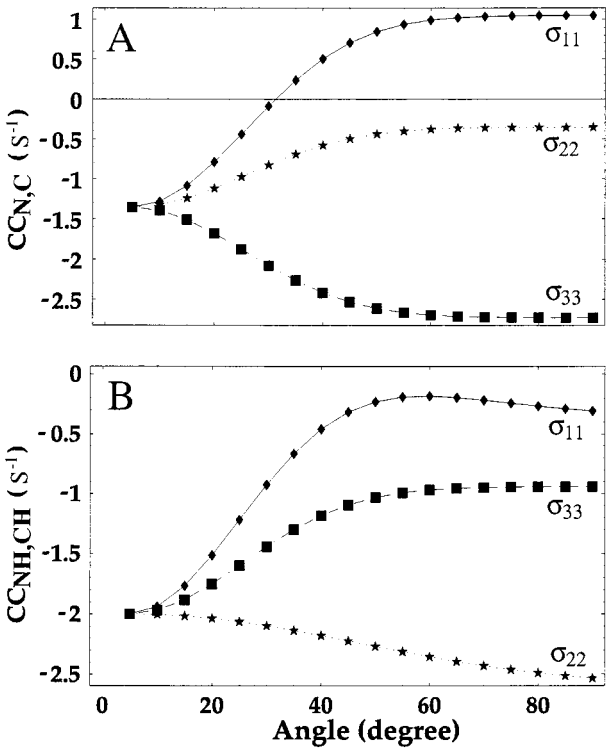

Figure 5. (A) A computation of the variations in $CC_{N,C}(0)$ cross-correlation rates with local anisotropic motions according eqs 2e, 5, 6, and 7. The following values were used for the calculations: the ^{13}CO chemical shielding sub tensors, ($\sigma_{11}-\sigma_{33}$) and ($\sigma_{22}-\sigma_{33}$) were set to −154 and −88 ppm, respectively;[29] the ^{15}N chemical shielding tensor was assumed axially symmetric with $\Delta\sigma_N = -170$ ppm and the corresponding angle θ_{11} defining the orientation of that tensor with the σ_{11} axis of the carbonyl tensor was set to 116°. (B) Computation of the variations of $CC_{NH,CH}(0)$ cross-correlation rates with local anisotropic motions according eqs 2d, 5, 6, and 7. Values used in the computation: r_{HN} and r_{HC} (see text) were set to 1.02 Å and 2.05 Å, respectively; the angle between the $^1H^N-^{15}N$ and $^1H^N-^{13}CO$ bond vectors was set to 35°. The diamonds, stars, and squares show the variation of the cross-correlation rate upon Gaussian rotational diffusion around vectors parallel to σ_{11}, σ_{22}, and σ_{33}, respectively. The angle reports motion over a range corresponding to ±1 standard deviation of the axial Gaussian distribution. The computations were made with the program Mathematica 3.0.

completely inexplicable variations in the $CC_{HN,CH}(0)$ cross-correlations rates. We may thus conclude that the measured experimental spread in both cross-correlation rates indicates the presence of extensive anisotropic local motions of the individual peptide planes. However, local motion of otherwise rigid peptide planes still cannot explain the very large values of cross-correlations rates observed for several residues. It is conceivable that the motions themselves cause transient distortions of the peptide plane geometry, thus transiently affecting tensor values which by itself can cause relaxative effects and increase the spread even further.[39] While it is thus currently difficult to separate the dynamic and structural contributions to the variations in CC_{NC} and $CC_{NH,CH}$ cross-correlation rates, it can be stated that our present data does disclose that the peptide plane geometry and dynamics is surprisingly heterogeneous for this enzyme. We are currently investigating other cross-correlations involving the different nuclei of the peptide plane in an effort to estimate the degree of local structural variability and to further characterize internal anisotropic motions.[40] At this stage we

(35) Bremi, T.; Brüschweiler, R. *J. Am. Chem. Soc.* **1997**, *119*, 6672−6673.
(36) Lienin, S. F.; Brutscher, B. R.; Brüschweiler, R.; Ernst, R. R. *J. Am. Chem. Soc.* **1998**, *120*, 9870−9879.
(37) Brunne, R. M.; Berndt, K. D.; Güntert, P.; Wüthrich, K.; Van Gunsteren, W. F. *Proteins, Struct., Funct., Genet.* **1995,** *23*, 49−62.
(38) Fadel, A. R.; Jin, D. Q.; Montelione, G. T.; Levy, R. M. *J. Biomol. NMR* **1995**, *6*, 221−226.
(39) Scheuer, C.; Skrynnikov, N. R.; Lienin, S. F.; Strausss, S. K.; Bruschweiler, R.; Ernst, R. R. *J. Am. Chem. Soc*. **1999**, *121*, 4242−4251.

cannot correlate the variations in $CC_{N,C}(0)$ (Figure 5a) and $CC_{NH,CH}(0)$ (Figure 5b) very well, especially for the C terminus of the protein. It is of interest to note that the active site of the enzyme, for which extensive ms dynamics has been measured as well (to be published), is located in this area.

The CSA−CSA cross-correlation does not depend on the distance between the nuclei involved but only on the possibility of creating a multiple-quantum coherence between them, just as other "remote" cross-correlations such as those reported by Reif et al.[15] If, for example, one would evolve the amide proton instead of the amide nitrogen together with ^{13}CO during the time period Δ in Figure 1B, one would obtain a spectrum where the cross-peak intensity ratio would be a measure of the $^1H^N$ and ^{13}CO CSA−CSA cross-correlation. Accordingly, one can devise a novel series of multiple-quantum experiments to measure "remote" CSA−CSA cross-correlations which, when taken all together, would allow a complete characterization of the local motions and their correlations, and at the same time provide useful structural information. In analogy with solid-state NMR studies on chemical shielding tensor orientations to derive dihedral angles,[41−44] for example, corresponding solution NMR multiple-quantum experiments to measure "remote" CSA−CSA cross-correlation can be designed and the resulting rates be correlated with dihedral angles. Another aspect of the CSA−CSA cross-correlations deserves particular attention for future applications. Recently, Pervushin et al. reported a very useful exploitation of the differential line broadening due to DD−CSA cross-correlation between $^1H^N$ and ^{15}N to attenuate the transverse relaxation (TROSY).[18,19] Considering the dependence of the CSA−CSA cross-correlation with the magnetic field (eq 2) one can exploit such a cross-correlation to attenuate transverse relaxation at high magnetic field and in situations where CSA is a dominant mechanism of nuclear spin relaxation.[27] We are currently investigating other situations were we can further exploit such possibilities.

Acknowledgment. We thank Dr. Guy Dodson for high-resolution X-ray crystal structure coordinates of binase. This work was supported by Grants MCB 9513355 and MCB 9814431 from the National Science Foundation. Dr. Kumar was supported by a stipend from Parke-Davis/Warner-Lambert corporation.

JA991155D

(40) Pang, Y.; Wang, L.; Pellecchia, M.; Kurochkin, A. V.; Zuiderweg, E. R. P. *J. Biomol. NMR*, in press.

(41) Schmidt-Rohr, K. *Macromolecules* **1996**, *29*, 3975−3981.

(42) Costa, P. R.; Gross, J. D.; Hong, M.; Griffing, R. G. *Chem. Phys. Lett.* **1997**, *280*, 95−103.

(43) Gregory, D. M.; Mehta, M. A.; Shiels, J. C.; Drobny, G. P. *J. Chem. Phys.* **1997**, *107*, 28−42.

(44) Hong, M.; Gross, J. D.; Hu, W.; Griffing, R. G. *J. Magn. Reson.* **1998**, *135*, 169−177.

(45) Piotto, M.; Saudek, V.; Sklenar, V. *J. Biomol. NMR* **1992**, *2*, 661−665.

(46) Kurochkin, A. V.; Kirpichniov, M. P.; Rüterjans, H. *Dokl. Biochem.* **1991**, *30*, 282−286.

(47) Barford, N. C. *Experimental Measurements: Precision, Error and Truth;* John Wiley and Sons: New York, 1967; pp. 36−37.